Epinephrine Modulates BCAM/Lu and ICAM-4 Expression on the Sickle Cell Trait Red Blood Cell Membrane

Jamie L. Maciaszek,[†] Biree Andemariam,[‡] Greg Huber,[§¶] and George Lykotrafitis[†*]

[†]Department of Mechanical Engineering, University of Connecticut, Storrs, Connecticut; [‡]Adult Sickle Cell Center, Lea Center for Hematologic Disorders, [§]Richard Berlin Center for Cell Analysis and Modeling, and [¶]Department of Cell Biology, University of Connecticut Health Center, Farmington, Connecticut

ABSTRACT Collapse and sudden death in physical training are the most serious complications of sickle cell trait (SCT). There is evidence that erythrocytes in SCT patients aggregate during strenuous exercise, likely because of adhesive interactions with the extracellular matrix (ECM) and endothelial cells, and because of their irregular viscoelastic properties. This results in inflammation, blood flow impairment, and vaso-occlusive events. However, the exact role of stress conditions and how they lead to these complications is virtually unknown. Using single-molecule atomic force microscopy experiments, we found that epinephrine, a hormone that is secreted under stressful conditions, increases both the frequency and strength of adhesion events between basal cell adhesion molecule (BCAM/Lu) and ECM laminin, and between intercellular adhesion molecule-4 (ICAM-4) and endothelial $\alpha_v\beta_3$, compared with nonstimulated SCT erythrocytes. Increases in adhesion frequency provide significant evidence of the role of epinephrine in BCAM/Lu-laminin and ICAM-4-$\alpha_v\beta_3$ bonding, and suggest mechanisms of vaso-occlusion during physical exertion in SCT.

INTRODUCTION

Sickle cell trait (SCT) is a risk factor for collapse and sudden death during physical training (1–7). SCT is characterized by the presence of both normal adult hemoglobin (HbA) and abnormal sickle hemoglobin (HbS) in the red blood cell (RBC, erythrocyte). SCT affects more than three million people in the United States, ~40–50 times more than sickle cell disease (SCD) (8). In HbS, the normal sequence *Val-His-Leu-Thr-Pro-**Glu**-Glu-Lys* is changed to *Val-His-Leu-Thr-Pro-**Val**-Glu-Lys*, with the amino acid valine substituted for glutamic acid in the β6 site. The replacement of two charged groups by two hydrophobic ones leads to polymerization of deoxygenated Hb and to the formation of stiff HbS fibers comprising a fibrous gel (9–11). Between 40% and 42% of the hemoglobin content of most individuals with SCT is HbS (12). In contrast to homozygous SCD, heterozygous SCT is traditionally regarded as a benign condition (13–15). However, during strenuous exercise, individuals can develop a syndrome resembling SCD, with vaso-occlusive events resulting from changes in the RBC morphology, viscoelasticity, and adhesion (1,2,6,16–19). Vaso-occlusion occurs in crises in which the arterial circulation is blocked at one or many sites, leading to organ damage and ischemic pain (20). Endothelial cell (EC) activation, cytoadherence, inflammation, and coagulation activation contribute to blood flow obstruction and play a critical role in the pathophysiology of vaso-occlusion (21–23).

It is known that SCD RBCs adhere abnormally to extracellular matrix (ECM) components and to ECs via changes in their adhesive interactions. Immature (reticulocytes) and mature erythrocytes express several adhesion receptors, including the Lutheran (Lu) blood group RBC antigen; basal cell adhesion molecule (BCAM), known as BCAM/Lu, which is a high-affinity laminin receptor; and intercellular adhesion molecule-4 (ICAM-4, LW glycoprotein), a receptor for a number of integrins (24).

Although it is known that epinephrine enhances SCD erythrocyte adhesion, the mechanism has not yet been quantitatively explored in SCT or SCD (25,26). Epinephrine is a hormone that is secreted from the adrenal medulla during periods of stress and strenuous exercise (27). Increased circulating levels of epinephrine act on the RBC β2-adrenergic receptor, thereby activating Gα_s proteins that stimulate adenylyl cyclase (AC). This enzyme catalyzes the conversion of adenosine triphosphate (ATP) to cyclic adenosine monophosphate (cAMP), leading to protein kinase A (PKA) activation, an intermediate step in the upregulation of BCAM/Lu- and ICAM-4-mediated adhesion (25,26,28). The interaction of BCAM/Lu with the α5 chain of laminin (LAMA5) on the ECM, as well as the interaction of ICAM-4 with the $\alpha_v\beta_3$ integrin on ECs, may contribute to vaso-occlusive events in SCD due to overexpression of BCAM/Lu and ICAM-4 on SCD RBCs in the presence and absence of epinephrine (24–26).

MATERIALS AND METHODS

Preparation of BCAM/Lu and ICAM-4 substrate

To attach purified CD239 (Sigma Aldrich, St. Louis, MO), commonly known as BCAM/Lu, onto a gold-coated mica substrate (Novascan Technologies, Ames, IA), we first incubated the substrate for 2 h in 50 mM mercaptoethanesulfonate. Mercaptoethanesulfonate was prepared by adding

Submitted February 10, 2011, and accepted for publication January 27, 2012.

*Correspondence: gelyko@engr.uconn.edu

Editor: Michael Edidin.

0006-3495/12/03/1137/7 $2.00

doi: 10.1016/j.bpj.2012.01.050

sodium 2-mercaptoethanesulfonate to equal parts ethanol and 18 MΩ water. The gold surface was allowed to dry, and then a drop of 1 μg/mL protein in phosphate-buffered saline (PBS) was added to the surface. After 20 min, the prepared gold surface was rinsed with PBS and a volume of PBS was added for experiments. The same method was employed to attach ICAM-4-1 (Sigma Aldrich, St. Louis, MO) to a gold-coated mica substrate.

Preparation of laminin and $\alpha_v\beta_3$ probes

Silicon nitride cantilevers were gently rinsed with ethanol and 18 MΩ water before they were placed into a clean, dry petri dish with 30 μL 3-aminopropy-triethoxysilane (APTES) and 10 μL triethylamine for 1 h. N_3-dPEG-NH_2 linker was prepared by adding dry methylene chloride (0.5 mL), triethylamine (7 μL), and 7.5 mg (7.5 μL) of N_3-dPEG-NH_2 linker (Quanta Biodesign, Powell, OH) to a small, dry, glass vial. The vial was sealed and inverted several times until all of the solid substances dissolved. After the atomic force microscopy (AFM) probes were tightly sealed with APTES for 1 h, they were removed and immediately added to the N_3-dPEG-NH_2 linker at 4°C. After 1 h, the probes were rinsed with methylene chloride, ethanol, and then 18 MΩ water. The probes were placed in a parafilm-coated dish with their tips pointed upward and inward in a circular manner. Then 50 μL of 250 μg/mL purified laminin α_5, clone 4C7 (Millipore, Temecula, CA), or 50 μL of 210 μg/mL purified human integrin $\alpha_v\beta_3$ (Millipore, Temecula, CA) were added to the center of the cantilevers, in contact with the probes. After 2 h, the AFM probes were rinsed with PBS buffer.

Erythrocyte preparation

The study included RBCs (Research Blood Components, Brighton, MA) obtained from an adult subject with SCT ($n = 1$) and a healthy adult subject ($n = 1$). An Institutional Review Board–approved consent form was obtained by the company for each donor that gave permission to use the acquired sample for research purposes. Sodium citrate anticoagulant was used, and the RBCs were used for experiments within 14 days of blood draw and maintained at 4°C before use. Cell age did not appear to have an effect on the data. Erythrocytes were diluted to a concentration of 50% in Alsever's solution (Sigma Aldrich, St. Louis, MO) and maintained in 5% CO_2 at 37°C before immobilization and experiments were performed.

Erythrocyte immobilization

Cells were immobilized on glass-bottomed petri dishes (MatTek, Ashland, MA) coated with poly-L-lysine (PLL) to increase cell adherence. Then 150 μl of 1 mg/mL PLL solution (Sigma Aldrich, St. Louis, MO) were allowed to adsorb for 5 min to a sterile glass surface, and excess solution was drained away. RBCs of 50% concentration in Alsever's solution were allowed to adhere to each PLL-coated glass surface for 10 min in the incubator (37°C and 5% CO_2). Unattached cells were removed by gentle rinsing of the surface with Alsever's solution at 25°C, and a volume of 3.0 mL Alsever's solution was added for experiments. For epinephrine-mediated adhesion experiments, a volume of 3.0 mL of 10 nM epinephrine (Sigma Aldrich, St. Louis, MO) was added.

AFM measurements

Adhesion maps and force-distance curves were obtained with the use of an Asylum MFP 3D-BIO atomic force microscope (Asylum Research, Santa Barbara, CA) equipped with a liquid-cell setup. A petri dish heater was employed to maintain the RBCs at physiological body temperature (37°C) during the experiments. The temperature inside the sample was controlled (± 0.1°C) via a closed-loop temperature control with an environmental controller (Asylum Research, Santa Barbara, CA). Baseline measurements were performed in Alsever's solution at 37°C. Epinephrine-mediated experiments were performed in a 10 nM epinephrine solution, using the Alsever's solution as the base, at 37°C. Unless otherwise specified, we recorded all force measurements with a loading rate of 24,000 pN/s, which we calculated by multiplying the tip retraction velocity (nm/s) by the spring constant of the cantilever (pN/nm).

The nominal spring constant k_c of the employed cantilever was 30 pN/nm, as provided by the manufacturer (Bruker Probes, Camarillo, CA). Exact values for the cantilever spring constants were obtained via a thermal noise-based method implemented by the manufacturer and were used in all calculations. We chose this cantilever stiffness because it is known that when $k_c > 10$ pN/nm, the soft linkage of the protein-protein interaction dominates the behavior of the cantilever-protein effective spring system (29). The approach and retraction velocities were held constant at 800 nm/s. The probes had nominal tip radii of 20 nm and a nominal angle of 20°, as provided by the manufacturer.

Statistical analysis

The reported adhesion interaction forces for the BCAM/Lu-laminin complex and ICAM-4-$\alpha_v\beta_3$ complex in the text are average values obtained via the Gaussian distribution. We assessed differences among the groups using the two-tailed t-test for independent samples to evaluate the effects of the SCT genotype and the epinephrine stimulation. The significance level was defined as $p < 0.05$. The statistical analyses were conducted with the Data Analysis Toolpack in Microsoft Excel (Microsoft, Redmond, WA).

RESULTS

Dynamics of the BCAM/Lu-laminin and ICAM-4-$\alpha_v\beta_3$ interaction

Direct measurements of the BCAM/Lu-laminin and ICAM-4-$\alpha_v\beta_3$ adhesive interactions were obtained via single-molecule force spectroscopy (30–32). Adhesive forces, defined as the maximum rupture force (Fig. 1 *B*) associated with the force-distance curves, were extracted from each of 1024 force curves that were acquired to determine the rupture force. Upon investigation of the dynamics of the BCAM/Lu-laminin interaction, force curves between the LAMA5 tip and the BCAM/Lu-coated substrate were recorded at various retraction rates. The mean adhesion force did not substantially depend on the loading rate applied during retraction, over the experimentally tested range (Fig. 1 *C*). The dynamics of the ICAM-4-$\alpha_v\beta_3$ interaction showed a similar trend. This observation, in contrast to the behavior of several other receptor-ligand complexes that usually show an increase in adhesion force with the logarithm of loading rate, indicates that the force measurements were performed close to thermodynamic equilibrium (33).

Interaction force of the BCAM/Lu-laminin and ICAM-4-$\alpha_v\beta_3$ pairs

For the BCAM/Lu-laminin pair, force-distance curves were recorded between the LAMA5 probe and the BCAM/Lu-coated substrate. Adhesive forces were extracted from each of the 1024 force curves acquired, and an average

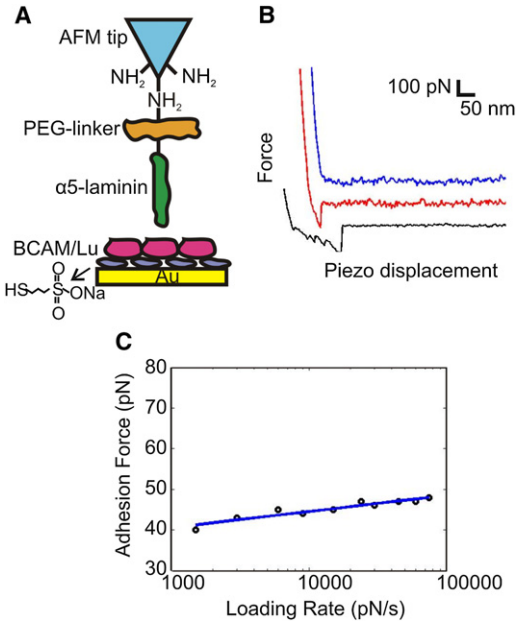

FIGURE 1 Strategy for measuring the BCAM/Lu-laminin binding force at the single-molecule level using AFM. (*A*) Schematic of the surface chemistry used to functionalize the AFM tip and substrate with LAMA5 and BCAM/Lu. A PEG-linker was attached to an AFM tip terminated with NH_2 groups, and BCAM/Lu was bound to a gold substrate via mercaptoethanesulfonate. (*B*) Force-distance curves are three representative examples obtained using independent tips and substrates. The uppermost (*blue*) curve demonstrates zero adhesive interaction, while the middle (*red*) and bottom (*black*) curves show rupture forces associated with adhesion events. (*C*) Dynamics of the BCAM/Lu-laminin interaction. Dependence of the adhesion force on the loading rate applied during retraction, measured between a LAMA5 tip and a BCAM/Lu substrate, while keeping the interaction time (0 s) and loading rate during approach (24000 pN/s) constant. The mean adhesion force does not notably change with the loading rate, indicating the measurements were performed close to thermodynamic equilibrium.

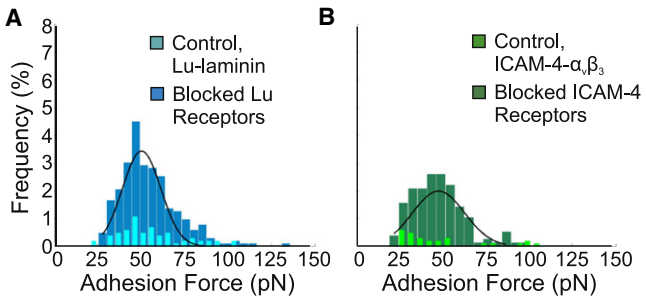

FIGURE 2 Measurement of the binding force of the BCAM/Lu-laminin and ICAM-4-$\alpha_v\beta_3$ complexes. (*A*) Adhesion force histogram obtained from 1024 force curves ($n = 1024$) measured in PBS between a LAMA5 tip and a BCAM/Lu substrate. The distribution of adhesion forces reveals a maximum value at 50 ± 11 pN as determined by a Gaussian fit. The frequency of adhesion events was 26%, as determined by the percentage of curves showing rupture forces. The overlay shows the adhesion force histogram ($n = 1024$) obtained after injection of free laminin (250 μg/mL) into the solution. The dramatic reduction of adhesion frequency and broadening of the distribution reflect the blocking of the BCAM/Lu receptors. (*B*) Adhesion force histogram obtained from 1024 force curves ($n = 1024$) measured in PBS between an integrin $\alpha_v\beta_3$ tip and a ICAM-4 substrate. The distribution of adhesion forces reveals a maximum value at 47 ± 15 pN as determined by a Gaussian fit. The frequency of adhesion events was 18%. The overlay shows the adhesion force histogram ($n = 1024$) obtained after injection of free integrin $\alpha_v\beta_3$ (210 μg/mL) into the solution. The dramatic reduction of adhesion frequency reflects the blocking of the ICAM-4 receptors.

rupture force of 50 ± 11 pN was obtained (Fig. 2 *A*). In AFM, one can determine the specificity of ligand-receptor binding by performing blocking experiments with free ligands, which are injected into the solution to block the receptor sites on the cell surface. Consequently, almost all specific recognition signals completely disappear and only occasional adhesion events are observed (30,34). We demonstrated the specificity of the interaction by performing experiments in 250 μg/mL laminin solution, thus blocking the BCAM/Lu receptors. By recording force-distance curves between the LAMA5 tip and the BCAM/Lu-coated substrate in the laminin solution, we were able to show that the percentage of curves exhibiting adhesion events reduced dramatically from 26% to 6% ($p < 10^{-6}$; Fig. 2 *A*). For the ICAM-4-$\alpha_v\beta_3$ pair, force-distance curves were recorded between the $\alpha_v\beta_3$ probe and the ICAM-4-coated substrate, resulting in an average rupture force of 47 ± 15 pN (Fig. 2 *B*). We demonstrated the specificity of the interaction by performing experiments in 210 μg/mL integrin $\alpha_v\beta_3$ solution, thus blocking the ICAM-4 receptors. The percentage of curves that showed adhesion events reduced dramatically from 18% to 3% ($p < 10^{-6}$; Fig. 2 *B*).

Nonstimulated SCT RBC adhesion to laminin and integrin $\alpha_v\beta_3$

In single erythrocytes we measured the effects of epinephrine on the bond strength and the frequency of binding events between 1), the BCAM/Lu antigen, expressed on the surface of SCT RBCs, and the laminin complex, expressed on the ECM; and 2), the ICAM-4 antigen expressed on the surface of SCT RBCs, and the $\alpha_v\beta_3$ integrin, expressed on ECs. We also measured the adhesion of nonstimulated SCT RBCs compared with nonstimulated wild-type (WT) RBCs. This method requires functionalization of the AFM probe (30–32,35) with LAMA5 or integrin $\alpha_v\beta_3$ to measure the interaction between the α5 chain of laminin and BCAM/Lu receptor expressed on the tested RBC (Fig. 3), or the interaction between integrin $\alpha_v\beta_3$ and ICAM-4 receptor expressed on the tested RBC. From these measurements, the distribution of the BCAM/Lu and ICAM-4 receptor on the RBC surface is also obtained. We placed the RBCs in an environment with a physiologically relevant level of epinephrine to explore the effects of the stress-induced epinephrine environment on the frequency and distribution of adhesive interactions.

To detect the distribution of the receptors on the cell surface, and to measure the physiologic BCAM/Lu-laminin

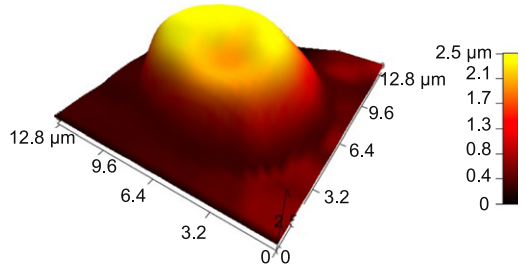

FIGURE 3 AFM topographic image of a SCT erythrocyte displaying the characteristic biconcave shape associated with healthy WT RBCs. This erythrocyte is a representative example of the cells that were scanned during experiments to map the distribution of BCAM/Lu and ICAM-4 receptors on human erythrocytes.

bond strength, we recorded spatially resolved adhesion maps using a LAMA5 tip over 1 μm $\times$ 1 μm areas. Adhesive forces were extracted from each of the 1024 force curves acquired from tests on $n = 6$ WT and $n = 6$ SCT erythrocytes. The average magnitude of the BCAM/Lu-laminin bond was the same for WT and SCT (Fig. 4 *A*) erythrocytes: 46 $\pm$ 6 pN and 46 $\pm$ 10 pN, respectively. This bond strength is also the same as the average rupture force of 50 $\pm$ 11 pN (Fig. 2 *A*) measured between a BCAM/Lu-coated gold substrate and a functionalized LAMA5 probe. The number of observed binding events, however, shows an increase from 10.42% to 16.89% ($p < 0.05$).

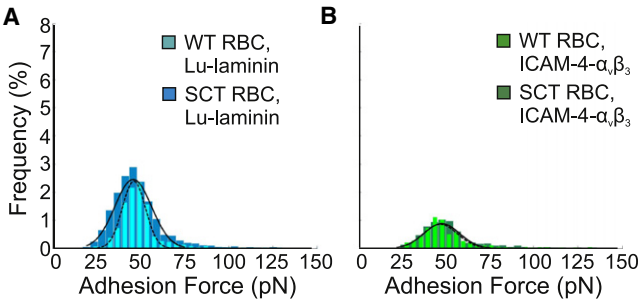

FIGURE 4 Measurement of the binding force of the BCAM/Lu-laminin and ICAM-4-$\alpha_v\beta_3$ complexes on erythrocytes. (*A*) Foreground: Adhesion force histogram obtained from 6144 force curves ($n = 6$ cells $\times$ 1024 force curves) measured in Alsever's solution between a LAMA5 tip and a WT RBC. The distribution of adhesion forces reveals a maximum value at 46 $\pm$ 6 pN, as determined by a Gaussian fit. Background: Adhesion force histogram obtained from 6144 force curves ($n = 6$ cells $\times$ 1024 force curves) obtained between a LAMA5 tip and a SCT RBC reveals a distribution of adhesion forces with a maximum value at 46 $\pm$ 10 pN. The frequency of adhesion events increased significantly from 10.42% on the WT RBC to 16.89% on the SCT RBC ($p < 0.05$). (*B*) Foreground: Adhesion force histogram obtained from 6144 force curves ($n = 6$ cells $\times$ 1024 force curves) measured in Alsever's solution between a $\alpha_v\beta_3$ tip and a WT RBC. The distribution of adhesion forces reveals a maximum value at 46 $\pm$ 10 pN, as determined by a Gaussian fit. Background: Adhesion force histogram ($n = 6$ cells $\times$ 1024 force curves) obtained between a $\alpha_v\beta_3$ tip and a SCT RBC reveals a distribution of adhesion forces with a maximum value at 47 $\pm$ 10 pN. There is a nonsignificant increase from 5.91% to 7.56% ($p > 0.05$) in the number of adhesion events.

For the measurements of the ICAM-4-$\alpha_v\beta_3$ pair bond strength and local distribution, we extracted adhesive forces from each of the 1024 force curves acquired from tests on $n = 6$ WT and $n = 6$ SCT erythrocytes. The average magnitude of the ICAM-4-$\alpha_v\beta_3$ bond was the same for WT and SCT (Fig. 4 *B*) erythrocytes: 46 $\pm$ 10 pN and 47 $\pm$ 10 pN, respectively. This bond strength is also nearly the same as the average rupture force of 47 $\pm$ 15 pN (Fig. 2 *B*) measured between an ICAM-4-coated gold substrate and a functionalized integrin $\alpha_v\beta_3$ probe. The number of observed binding events showed an insignificant increase from 5.91% to 7.56% ($p > 0.05$).

Epinephrine-stimulated SCT RBC adhesion to laminin and integrin $\alpha_v\beta_3$

To test the hypothesis that an increase in epinephrine levels results in an increase in the frequency of adhesive interactions, we employed a similar approach. Treatment of WT RBCs with 10 nM epinephrine, a physiologically relevant level, induced an insignificant increase from 10.42% to 14.86% ($p > 0.05$) in the frequency of BCAM/Lu-laminin binding events ($n = 6$; Fig. 5 *A*), and an insignificant increase from 5.91% to 8.99% ($p > 0.05$) in the frequency

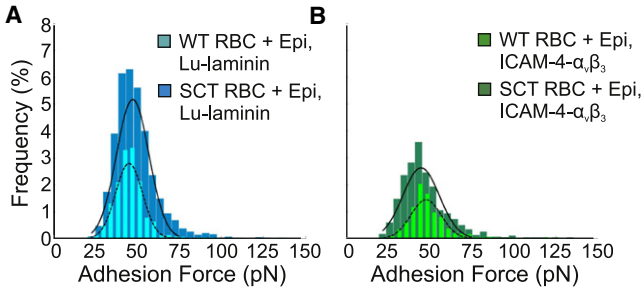

FIGURE 5 Measurement of the physiologic implications of epinephrine-stimulated adhesion. (*A*) Foreground: Adhesion force histogram ($n = 6$ cells $\times$ 1024 force curves) obtained in 10 nM epinephrine between a LAMA5 tip and a WT RBC reveals a distribution of adhesion forces with a maximum value at 45 $\pm$ 8 pN, comparable to the baseline value. The frequency of adhesion events increased from 10.42% to 14.86% ($p > 0.05$) as compared with baseline measurements of WT RBCs. Background: Adhesion force histogram ($n = 6$ cells $\times$ 1024 force curves) obtained between a LAMA5 tip and an SCT RBC. The frequency of adhesion events increased significantly from 16.89% to 35.04% ($p < 0.01$) as compared with baseline measurements of SCT RBCs. The distribution reveals a maximum value at 48 $\pm$ 10 pN, comparable to the baseline SCT value. (*B*) Foreground: Adhesion force histogram ($n = 6$ cells $\times$ 1024 force curves) obtained in 10 nM epinephrine between an integrin $\alpha_v\beta_3$ tip and a WT RBC reveals a distribution of adhesion forces with a maximum value at 48 $\pm$ 9 pN, comparable to the baseline value. The frequency of adhesion events increased insignificantly from 5.91% to 8.99% ($p > 0.05$) as compared with baseline measurements of WT RBCs. Background: Adhesion force histogram ($n = 6$ cells $\times$ 1024 force curves) obtained between an integrin $\alpha_v\beta_3$ tip and an SCT RBC. The frequency of adhesion events increased from 7.56% to 19.89% ($p < 0.05$) as compared with baseline measurements of SCT RBCs. The distribution reveals a maximum value at 45 $\pm$ 11 pN, comparable to the baseline value.

of ICAM-4-$\alpha_v\beta_3$ binding events ($n = 6$; Fig. 5 *B*). There was no notable increase in the bond strength of either pair with epinephrine stimulation. The specificity of the BCAM/Lu-laminin interaction was validated via blocking experiments (see Fig. S1 in the Supporting Material). By recording force-distance curves between a LAMA5 tip and WT RBCs in Alsever's solution, we found that the percentage of curves that showed adhesion events reduced dramatically from 10.42% to 0.52% ($p < 0.001$).

Treatment of SCT RBCs ($n = 6$) with epinephrine induced an increase in the frequency of BCAM/Lu-laminin binding events from 16.89% to 35.04% ($p < 0.01$; Fig. 5 *A*). In Fig. 5 *A* the distribution of the WT RBCs with epinephrine is overlaid on the distribution of the SCT RBCs with epinephrine to demonstrate the broadened variability of the Lu/BCAM-laminin adhesion force on the treated SCT erythrocytes. Treatment of SCT RBCs ($n = 6$) with epinephrine induced an increase in the frequency of ICAM-4-$\alpha_v\beta_3$ binding events from 7.56% to 19.89% ($p < 0.05$; Fig. 5 *B*). The distribution of the WT RBCs with epinephrine is overlaid on the distribution of the SCT RBCs with epinephrine in Fig. 5 *D* to demonstrate the broadened variability of the ICAM-4-$\alpha_v\beta_3$ adhesion force on the treated SCT erythrocytes.

Of note, the 1 μm $\times$ 1 μm spatially-resolved adhesion maps reveal that the BCAM/Lu-mediated laminin binding activity is not homogeneously distributed over the SCT RBC surface, but rather is concentrated on nanodomains. These nanodomains, often attributed to membrane rafts, are only observed on SCT RBCs ($n = 6$) in the presence of epinephrine (Fig. 6 *D*). In contrast, WT RBCs ($n = 6$) stimulated with epinephrine (Fig. 6 *C*) show a nearly homogeneous distribution of BCAM/Lu receptors. Furthermore, ICAM-4 receptor nanodomains are also observed, to a lesser degree, on the SCT RBC ($n = 6$) surface in the presence of epinephrine (Fig. 6 *H*), with a heterogeneous receptor distribution on the WT RBC ($n = 6$) stimulated with epinephrine (Fig. 6 *G*). In the nonstimulated environment, both WT (Fig. 6, *A* and *E*) and SCT (Fig. 6, *B* and *F*) RBCs maintain a homogeneous distribution of BCAM/Lu and ICAM-4 receptors.

DISCUSSION

Although it is known that the BCAM/Lu-laminin and ICAM-4-$\alpha_v\beta_3$ binding complexes contribute to SCD vaso-occlusion, the quantitative characteristics of these adhesion interactions have not been explored in SCD or SCT erythrocytes. In WT RBCs and SCT RBCs, the magnitude of the BCAM/Lu-laminin binding complex (46 $\pm$ 6 pN and 46 plusmn; 10 pN, respectively) is equal to the average rupture force of 50 $\pm$ 11 pN recorded between a functionalized laminin probe and a BCAM/Lu-coated gold substrate. In WT RBCs and SCT RBCs, the magnitude of the ICAM-4-$\alpha_v\beta_3$ binding complex (46 $\pm$ 10 pN and 47 $\pm$ 10 pN, respectively) is nearly the same as the average rupture force of 47 $\pm$ 15 pN recorded between a functionalized integrin $\alpha_v\beta_3$ probe and an ICAM-4-coated gold substrate.

Interactions of receptor molecule cytoplasmic domains with the cytoskeleton can play critical roles in adjusting receptor function. It was previously determined that BCAM/Lu has a high degree of connectivity to the erythrocyte membrane cytoskeleton via erythroid spectrin (36,37). Of importance, disruption of the BCAM/Lu-spectrin linkage is accompanied by enhanced cell adhesion to laminin (37). A major finding of this study is that BCAM/Lu adhesion events in SCT erythrocytes increased ($p < 0.05$) compared with the WT. It is known that Hb interacts with the spectrin network via band 3 (38,39), and the introduction of HbS was recently found to have an effect on the mechanical properties of SCT erythrocytes (40). We conjecture that HbS partially disrupts the spectrin network via its interaction with band 3, indirectly disrupting the BCAM/Lu-spectrin linkage. This results in increased diffusion and aggregation, and thus significantly enhanced SCT RBC adhesion to ECM laminin.

Epinephrine, acting through the β2-adrenergic receptor, increases Lu-laminin α5 sickle-mediated red cell binding

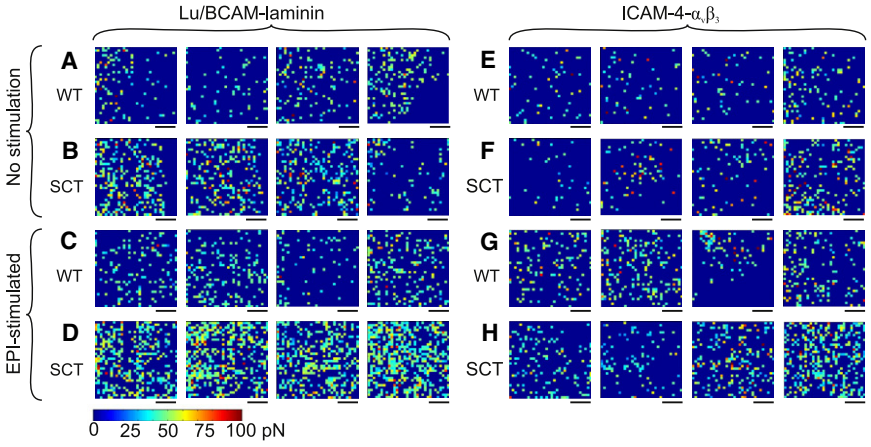

FIGURE 6 Distribution of BCAM/Lu and ICAM-4 on the surface of WT RBCs and SCT RBCs using different probes and cell preparations. (*A* and *B*) Adhesion force maps (color scale as shown) recorded with LAMA5 functionalized probes over WT RBCs (*A*) and SCT RBCs (*B*). (*C* and *D*) Adhesion force maps recorded with LAMA5 tips over WT RBCs (*C*) and SCT RBCs (*D*) in 10 nM epinephrine. (*E* and *F*) Adhesion force maps recorded with integrin $\alpha_v\beta_3$ probes over WT RBCs (*E*) and SCT RBCs (*F*). (*G* and *H*) Adhesion force maps recorded with integrin $\alpha_v\beta_3$ tips over WT RBCs (*G*) and SCT RBCs (*H*) in 10 nM epinephrine. Scale bars: 250 nm.

via a cAMP- and PKA-dependent signaling pathway (25). Further, the Lu cytoplasmic tail is phosphorylated in epinephrine-stimulated sickle cells, which may be a critical factor in sickle RBCs' enhanced adhesion to laminin (41). The BCAM cytoplasmic tail, which lacks the last 40 amino acids of the sequence, does not undergo phosphorylation. It was previously shown that PKA-mediated phosphorylation of the Lu glycoprotein at Ser-621 positively regulates the adhesion function of Lu under flow conditions (41). Although the molecular basis for the resulting increased adhesion is not yet understood, it was hypothesized that phosphorylation of the Lu cytoplasmic tail weakens its interaction with spectrin, enabling the freely-floating transmembrane Lu molecules to cluster and thereby generate a larger adhesive force. A major result of this study is the mapping of Lu nanodomains on epinephrine-stimulated SCT erythrocytes, accompanied by an increase in the frequency of binding events ($p < 0.01$) from the baseline SCT erythrocytes. The significant broadening of the bond magnitude distribution agrees with the aggregation of receptors into nanodomains detected in Fig. 6 *D*. Although the frequency of adhesive interactions increases on the WT RBC in the stress-induced epinephrine environment, this increase (from 10.42% to 14.86%) is not significant, and receptor clustering is not observed (Fig. 6 *C*). This observation strengthens our conjecture that HbS disrupts the spectrin network, resulting in aggregation of BCAM/Lu receptors in SCT RBCs. Of note, receptor aggregation is not detected in the case of SCT RBCs without epinephrine (Fig. 6 *B*).

ICAM-4-mediated binding to ECs and leukocytes is also activated by epinephrine via stimulation of the β2-adrenergic receptor, which triggers a cAMP- and PKA-dependent signaling pathway (42). In addition, ICAM-4 on epinephrine-stimulated sickle cells undergoes a significant increase in serine phosphorylation, which may be a critical factor in sickle RBCs' enhanced adhesion to endothelial integrin $\alpha_v\beta_3$ (26). It has been hypothesized that phosphorylation-induced changes in the ICAM-4 cytoplasmic domain cause a conformational change in its extracellular domain, thereby generating a larger adhesive force. We observed an increase in the frequency of binding events ($p < 0.05$) from the baseline SCT erythrocytes (Fig. 5 *D*) on epinephrine-stimulated SCT erythrocytes. Another important result of this study is the quantification of the insignificant increase ($p > 0.05$) of ICAM-4-$\alpha_v\beta_3$ adhesion events on the WT RBCs in the stress-induced epinephrine environment (Fig. 5 *B*). This is consistent with the fact that minimal ICAM-4 phosphorylation occurs in WT RBCs, due to an age-related reduction in the cells' ability to produce cAMP and thereby enhance PKA activity in response to stimulation (25,43,44). Although in this study we tested the effect of epinephrine on single-molecule adhesion interactions that are thought to contribute to vascular blockage in sickle cell vaso-occlusion, epinephrine has also been found to work by increasing RBC trapping in the spleen and liver (42,45).

CONCLUSIONS

The observed increases in adhesion frequency along with the detected receptor aggregation into nanodomains provide significant evidence of the role of epinephrine in enhancing BCAM/Lu-laminin and ICAM-4-$\alpha_v\beta_3$ bond interactions. These findings suggest a mechano-adhesive role for epinephrine in the pathophysiology of vaso-occlusive incidents related to sudden death in SCT individuals during strenuous exercise.

SUPPORTING MATERIAL

A figure is available at http://www.biophysj.org/biophysj/supplemental/S0006-3495(12)00167-1.

B.A. thanks the Connecticut Institute for Clinical and Translational Science (K12 Award) and the Lea Foundation for Leukemia Research. B.A., G.H., and G.L. thank the Connecticut Institute for Clinical and Translational Science (CICATS) and Connecticut Sickle Cell Translational Science (CTS•CTS) consortium for support.

This study was supported by the American Heart Association (fellowship 11PRE7280009 to J.L.M.) and the Richard Berlin Center for Cell Analysis and Modeling (G.H.).

REFERENCES

1. Jones, Sr., S. R., R. A. Binder, and E. M. Donowho, Jr. 1970. Sudden death in sickle-cell trait. *N. Engl. J. Med.* 282:323–325.
2. Kark, J. A., D. M. Posey, …, C. J. Ruehle. 1987. Sickle-cell trait as a risk factor for sudden death in physical training. *N. Engl. J. Med.* 317:781–787.
3. Tsaras, G., A. Owusu-Ansah, …, Y. Amoateng-Adjepong. 2009. Complications associated with sickle cell trait: a brief narrative review. *Am. J. Med.* 122:507–512.
4. Mitchell, B. L. 2007. Sickle cell trait and sudden death—bringing it home. *J. Natl. Med. Assoc.* 99:300–305.
5. Sears, D. A. 1978. The morbidity of sickle cell trait: a review of the literature. *Am. J. Med.* 64:1021–1036.
6. Kark, J. A., and F. T. Ward. 1994. Exercise and hemoglobin S. *Semin. Hematol.* 31:181–225.
7. Miller, F. A., M. Paynter, …, P. Chakraborty. 2010. Understanding sickle cell carrier status identified through newborn screening: a qualitative study. *Eur. J. Hum. Genet.* 18:303–308.
8. Kark, J. A. 2000. Sickle Cell Trait. Center for Sickle Cell Disease, Howard University School of Medicine, Washington, DC.
9. Ferrone, F. A. 2004. Polymerization and sickle cell disease: a molecular view. *Microcirculation.* 11:115–128.
10. Noguchi, C. T., and A. N. Schechter. 1985. Sickle hemoglobin polymerization in solution and in cells. *Annu. Rev. Biophys. Biophys. Chem.* 14:239–263.
11. Li, H., and G. Lykotrafitis. 2011. A coarse-grain molecular dynamics model for sickle hemoglobin fibers. *J. Mech. Behav. Biomed. Mater.* 4:162–173.
12. Wells, I. C., and H. A. Itano. 1951. Ratio of sickle-cell anemia hemoglobin to normal hemoglobin in sicklemics. *J. Biol. Chem.* 188:65–74.
13. Pauling, L., H. A. Itano, I. C. Wells…, 1949. Sickle cell anemia a molecular disease. *Science.* 110:543–548.
14. Neel, J. V. 1949. The inheritance of sickle cell anemia. *Science.* 110:64–66.

15. Strasser, B. J. 1999. Perspectives: molecular medicine. "Sickle cell anemia, a molecular disease". *Science.* 286:1488–1490.

16. Martin, T. W., I. M. Weisman, …, S. R. Stephenson. 1989. Exercise and hypoxia increase sickling in venous blood from an exercising limb in individuals with sickle cell trait. *Am. J. Med.* 87:48–56.

17. Connes, P., O. Hue, …, M. D. Hardy-Dessources. 2008. Blood rheology abnormalities and vascular cell adhesion mechanisms in sickle cell trait carriers during exercise. *Clin. Hemorheol. Microcirc.* 39:179–184.

18. Connes, P., H. Reid, …, O. Hue. 2008. Physiological responses of sickle cell trait carriers during exercise. *Sports Med.* 38:931–946.

19. Tripette, J., P. Connes, …, M. D. Hardy-Dessources. 2010. Red blood cell deformability and aggregation, cell adhesion molecules, oxidative stress and nitric oxide markers after a short term, submaximal, exercise in sickle cell trait carriers. *Clin. Hemorheol. Microcirc.* 45:39–52.

20. Stuart, M. J., and R. L. Nagel. 2004. Sickle-cell disease. *Lancet.* 364:1343–1360.

21. Brittain, H. A., J. R. Eckman, …, T. M. Wick. 1993. Thrombospondin from activated platelets promotes sickle erythrocyte adherence to human microvascular endothelium under physiologic flow: a potential role for platelet activation in sickle cell vaso-occlusion. *Blood.* 81:2137–2143.

22. Ballas, S. K., and N. Mohandas. 1996. Pathophysiology of vaso-occlusion. *Hematol. Oncol. Clin. North Am.* 10:1221–1239.

23. Conran, N., C. F. Franco-Penteado, and F. F. Costa. 2009. Newer aspects of the pathophysiology of sickle cell disease vaso-occlusion. *Hemoglobin.* 33:1–16.

24. Telen, M. J. 2007. Role of adhesion molecules and vascular endothelium in the pathogenesis of sickle cell disease. *Hematology Am. Soc. Hematol. Educ. Program.* 2007:84–90.

25. Hines, P. C., Q. Zen, …, L. V. Parise. 2003. Novel epinephrine and cyclic AMP-mediated activation of BCAM/Lu-dependent sickle (SS) RBC adhesion. *Blood.* 101:3281–3287.

26. Zennadi, R., P. C. Hines, …, M. J. Telen. 2004. Epinephrine acts through erythroid signaling pathways to activate sickle cell adhesion to endothelium via LW-$\alpha v\beta 3$ interactions. *Blood.* 104:3774–3781.

27. Kjaer, M. 1998. Adrenal medulla and exercise training. *Eur. J. Appl. Physiol. Occup. Physiol.* 77:195–199.

28. Kaul, D. K. 2004. "Stress" and sickle red cell adhesion. *Blood.* 104:3425–3426.

29. Evans, E. 2001. Probing the relation between force—lifetime—and chemistry in single molecular bonds. *Annu. Rev. Biophys. Biomol. Struct.* 30:105–128.

30. Dufrêne, Y. F., and P. Hinterdorfer. 2008. Recent progress in AFM molecular recognition studies. *Pflugers Arch.* 456:237–245.

31. Dupres, V., F. D. Menozzi, …, Y. F. Dufrêne. 2005. Nanoscale mapping and functional analysis of individual adhesins on living bacteria. *Nat. Methods.* 2:515–520.

32. Lim, T. S., S. R. K. Vedula, …, C. T. Lim. 2008. Single-molecular-level study of claudin-1-mediated adhesion. *Langmuir.* 24:490–495.

33. Auletta, T., M. R. de Jong, …, L. Kuipers. 2004. β-Cyclodextrin host-guest complexes probed under thermodynamic equilibrium: thermodynamics and AFM force spectroscopy. *J. Am. Chem. Soc.* 126:1577–1584.

34. Acharya, K., C. W. Lang, and L. F. Ross. 2009. A pilot study to explore knowledge, attitudes, and beliefs about sickle cell trait and disease. *J. Natl. Med. Assoc.* 101:1163–1172.

35. Lee, S., J. Mandic, and K. J. Van Vliet. 2007. Chemomechanical mapping of ligand-receptor binding kinetics on cells. *Proc. Natl. Acad. Sci. USA.* 104:9609–9614.

36. Parsons, S. F., G. Lee, …, J. A. Chasis. 2001. Lutheran blood group glycoprotein and its newly characterized mouse homologue specifically bind $\alpha 5$ chain-containing human laminin with high affinity. *Blood.* 97:312–320.

37. An, X. L., E. Gauthier, …, J. A. Chasis. 2008. Adhesive activity of Lu glycoproteins is regulated by interaction with spectrin. *Blood.* 112:5212–5218.

38. Fortier, N., L. M. Snyder, …, N. Mohandas. 1988. The relationship between in vivo generated hemoglobin skeletal protein complex and increased red cell membrane rigidity. *Blood.* 71:1427–1431.

39. Snyder, L. M., L. Leb, …, N. L. Fortier. 1983. Irreversible spectrin-haemoglobin crosslinking in vivo: a marker for red cell senescence. *Br. J. Haematol.* 53:379–384.

40. Maciaszek, J. L., and G. Lykotrafitis. 2011. Sickle cell trait human erythrocytes are significantly stiffer than normal. *J. Biomech.* 44: 657–661.

41. Gauthier, E., C. Rahuel, …, C. Le Van Kim. 2005. Protein kinase A-dependent phosphorylation of Lutheran/basal cell adhesion molecule glycoprotein regulates cell adhesion to laminin $\alpha 5$. *J. Biol. Chem.* 280:30055–30062.

42. Zennadi, R., B. J. Moeller, …, M. J. Telen. 2007. Epinephrine-induced activation of LW-mediated sickle cell adhesion and vaso-occlusion in vivo. *Blood.* 110:2708–2717.

43. Porzig, H., R. Gutknecht, …, K. Thalmeier. 1995. G-protein-coupled receptors in normal human erythroid progenitor cells. *Naunyn Schmiedebergs Arch. Pharmacol.* 353:11–20.

44. Baumann, R., C. Blass, …, S. Dragon. 1999. Ontogeny of catecholamine and adenosine receptor-mediated cAMP signaling of embryonic red blood cells: role of cGMP-inhibited phosphodiesterase 3 and hemoglobin. *Blood.* 94:4314–4320.

45. Ebert, E. C., M. Nagar, and K. D. Hagspiel. 2010. Gastrointestinal and hepatic complications of sickle cell disease. *Clin. Gastroenterol. Hepatol.* 8:483–489, quiz e70.